

# Ephrin-A2 and -A5 Influence Patterning of Normal and Novel Retinal Projections to the Thalamus: Conserved Mapping Mechanisms in Visual and Auditory Thalamic Targets

CHARLENE A. ELLSWORTH,<sup>1</sup> ALVIN W. LYCKMAN,<sup>1,2</sup> DAVID A. FELDHEIM,<sup>3</sup>  
JOHN G. FLANAGAN,<sup>4</sup> AND MRIGANKA SUR<sup>1,2\*</sup>

<sup>1</sup>Department of Brain and Cognitive Sciences, Massachusetts Institute of Technology, Cambridge, Massachusetts 02139

<sup>2</sup>The Picower Center for Learning and Memory, Massachusetts Institute of Technology, Cambridge, Massachusetts 02139

<sup>3</sup>Molecular, Cell, and Developmental Biology, University of California, Santa Cruz, Santa Cruz, California 95064

<sup>4</sup>Department of Cell Biology and Program in Neuroscience, Harvard Medical School, Boston, Massachusetts 02115

---

---

## ABSTRACT

Sensory axons are targeted to modality-specific nuclei in the thalamus. Retinal ganglion cell axons project retinotopically to their principal thalamic target, the dorsal lateral geniculate nucleus (LGd), in a pattern likely dictated by the expression of molecular gradients in the LGd. Deafferenting the auditory thalamus induces retinal axons to innervate the medial geniculate nucleus (MGN). These retino-MGN projections also show retinotopic organization. Here we show that ephrin-A2 and -A5, which are expressed in similar gradients in the MGN and LGd, can be used to pattern novel retinal projections in the MGN. As in the LGd, retinal axons from each eye terminate in discrete eye-specific zones in the MGN of rewired wild-type and ephrin-A2/A5 knockout mice. However, ipsilateral eye axons, which arise from retinal regions of high EphA5 receptor expression and represent central visual field, terminate in markedly different ways in the two mice. In rewired wild-type mice, ipsilateral axons specifically avoid areas of high ephrin expression in the MGN. In rewired ephrin knockout mice, ipsilateral projections shift in location and spread more broadly, leading to an expanded representation of the ipsilateral eye in the MGN. Similarly, ipsilateral projections to the LGd in ephrin knockout mice are shifted and are more widespread than in the LGd of wild-type mice. In the MGN, as in the LGd, terminations from the two eyes show little overlap even in the knockout mice, suggesting that local interocular segregation occurs regardless of other patterning determinants. Our data demonstrate that graded topographic labels, such as the ephrins, can serve to shape multiple related aspects of afferent patterning, including topographic mapping and the extent and spread of eye-specific projections. Furthermore, when mapping labels and other cues are expressed in multiple target zones, novel projections are patterned according to rules that operate in their canonical targets. *J. Comp. Neurol.* 488:140–151, 2005. © 2005 Wiley-Liss, Inc.

**Indexing terms:** topographic maps; eye-specific segregation; cross-modal plasticity; medial geniculate nucleus; lateral geniculate nucleus

---

---

Under certain experimental conditions, inputs of one modality can be induced to innervate thalamic nuclei of a different modality. Comparisons of projections in normal targets with those in novel targets should provide insight on how afferent and target-derived factors influence the development of modality-specific patterns. The lateral geniculate nucleus (LGN, including its dorsal and ventral divisions, LGd and LGv, respectively) is the primary thalamic recipient of visual fibers from retinal ganglion cell-axons, whereas the medial geniculate nucleus (MGN) is

---

Grant sponsor: National Institutes of Health; Grant number: EY11512 (to M.S.); Grant number: EY15068 (to M.S.).

\*Correspondence to: Mriganka Sur, Department of Brain and Cognitive Sciences, E25-235, Massachusetts Institute of Technology, Cambridge, MA 02139. E-mail: msur@mit.edu

Received 8 December 2003; Revised 27 July 2004; Accepted 14 February 2005

DOI 10.1002/cne.20602

Published online in Wiley InterScience (www.interscience.wiley.com).

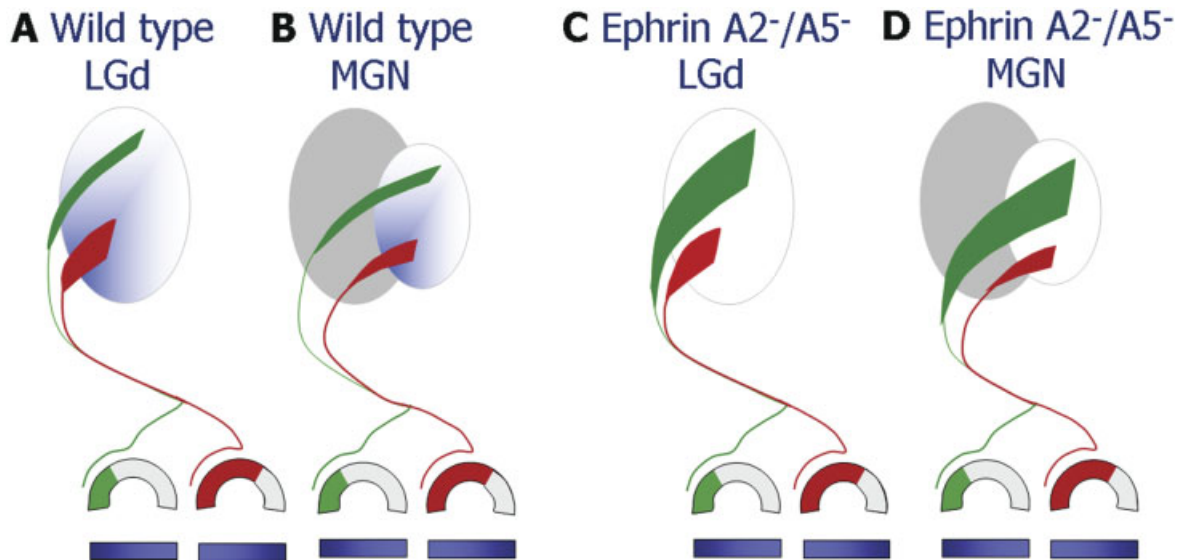


Fig. 1. Schematic representation of Eph/ephrin interactions in shaping normal and novel retinal projections in wild-type (A,B) and ephrin-A2/A5 knockout (C,D) mice. Contralateral projections are labeled in red; ipsilateral projections are labeled in green. Ephrin expression is represented by the blue gradient within the target nuclei, whereas Eph receptor expression is depicted by the green gradient under each retina. A: In wild-type mice, ipsilateral axons arise from the temporal retina and express high levels of EphA5 receptor. As a result, these axons target regions of the dorsal lateral geniculate

nucleus (LGd) with low ephrin expression. B: A similar ephrin gradient is also apparent in the medial geniculate nucleus (MGN). As a result of these parallel ephrin gradients, eye-specific projections are similar in the LGN and rewired MGN: in rewired wild-type mice, ipsilateral retino-MGN projections target regions of the MGN with low ephrin expression. C,D: In ephrin knockout mice, ipsilateral axons still show high EphA5 receptor expression but target broader regions of the LGN and MGN. Ipsilateral axons spread ventrally in both the LGN (C) and the rewired MGN (D) of ephrin knockout mice.

the principal target of auditory fibers from the inferior colliculus. Surgical deafferentation of the MGN in neonatal animals induces axons of retinal ganglion cells to innervate this nucleus (Schneider, 1973; Sur et al., 1988; Lyckman et al., 2001; Sur and Leamy, 2001). Similarly, deafferentation of the ventrobasal nucleus (VB), which normally receives somatosensory input, also induces aberrant visual innervation. Retino-MGN and retino-VB projections have features that are characteristic of retino-LGN projections, such as retinotopy and local eye-specific segregation (Frost, 1981; Angelucci et al., 1997, 1998). Auditory cortex that develops with visual input also has a retinotopic map of visual space, as well as orientation-selective cells and an orientation map (Roe et al., 1990; Sharma et al., 2000; Sur, 2004).

In the visual system, retinotopic ordering of inputs to visual targets depends on ephrin-Eph interactions (O'Leary and McLaughlin, 2005). Rodent retinal ganglion cells show a graded pattern of expression for the EphA5 receptor (Feldheim et al., 1998), whereas the LGd and superior colliculus express a gradient of the ligands ephrin-A2 and -A5. Repulsive interactions mediated by the EphA5 receptor on retinal ganglion cell axons in the presence of these dual ephrin-A gradients are essential to the development of retinotopic maps in both visual targets (Cheng et al., 1995; Drescher et al., 1995; Monschau et al., 1997; Feldheim et al., 1998, 2000, 2004; Frisen et al., 1998; Yates et al., 2001; Hansen et al., 2004; Reber et al., 2004; see also Monnier et al., 2002). Several members of the ephrin family are differentially expressed in the developing thalamus (Feldheim et al., 1998; Vanderhaeghen et al., 2000; Nakagawa et al., 2000; Lyckman et al., 2001; Williams et al., 2003). We previously reported an ephrin A gra-

dent in the MGN that is similar in orientation and expression level to that in the LGd (Lyckman et al., 2001). Here we asked whether ephrin-A gradients regulate the patterning of a surgically induced retino-MGN projection, analogous to their function in normal visual targets.

In rodents, ipsilateral axons (which represent central, binocular visual field) arise from cells in the ventrotemporal retina, a region with high EphA5 receptor expression. These axons may be especially sensitive to the parallel ephrin gradients in the LGd and MGN, targeting cells with low ephrin expression in both nuclei (Fig. 1A,B). If the ephrin gradient directly contributes to retino-MGN organization, we would expect ipsilateral patterning in the MGN to be different in wild-type and ephrin knockout mice. Furthermore, we would expect that any differences we see between the mice should be similar in the MGN and LGd (Fig. 1C,D). We show here that ipsilateral retino-MGN projections preferentially target areas of the MGN that show low ephrin expression in normal mice, whereas in ephrin knockout mice they are more extensive and have greater topographic spread than in wild-type mice. The changes in the patterning of the retino-MGN projection are comparable to those for the retino-LGd projection. Despite changes in the extent of eye-specific layers, the segregation of eye-specific inputs is maintained in the knockout mice, in the LGd and rewired MGN. These data suggest that guidance interactions mediated by relatively few receptor-ligand systems have important consequences for afferent patterning in multiple thalamic nuclei, including normal and novel targets of retinal axons.

## MATERIALS AND METHODS

### Animals

Surgeries were performed on wild-type 129/SvEv mice (Taconic Farms, Germantown, NY) and on ephrin-A2/A5 double knockout mice that were bred and maintained in our in-house colony (Division of Comparative Medicine, MIT). The ephrin-A2/A5 double knockout mouse (Feldheim et al., 2000) was generated by crossing a homozygous ephrin-A2 knockout in a pure 129/SvEv background with a homozygous ephrin-A5 knockout in a mixed Swiss-Webster/C57BL/6 background (Frisen et al., 1998). Live animal procedures were approved by the Committee on Animal Care at MIT and conformed to National Institutes of Health guidelines.

### Rewiring surgery

129/SvEv and ephrin-A2/A5 knockout mice were anesthetized 1 day after birth by deep hypothermia. By using high-temperature microcautery, we lesioned the left superior colliculus and the left inferior colliculus and severed the left brachium of the inferior colliculus with an 18-gauge needle. These combined procedures effectively deafened the left MGN, by removing ipsilateral inputs that arise in the inferior colliculus and ascend through the brachium of the inferior colliculus, as well as contralateral inputs that cross the midline at the level of the superior colliculus (Angelucci et al., 1998; Lyckman et al., 2001). Pups were revived under a heat lamp and were reared to adulthood.

### Ephrin-A and EphA expression

Expression patterns of ephrin-A proteins and EphA receptor tyrosine kinases were obtained by staining with alkaline phosphatase (AP)-coupled affinity probes (Flanagan et al., 2000). For ephrin-A staining of the thalamus, we used 100- $\mu$ m vibrotome sections from P0 mouse brains, unperfused and fixed for 20 minutes in paraformaldehyde. For Eph-A staining of the retina, we used 20- $\mu$ m whole-mount cryostat sections, fixed with paraformaldehyde for 15 seconds. Sections were incubated with ephrin-A5-coupled AP or EphA3-coupled AP in HBAH buffer [Hanks balanced salt solution, bovine serum albumin (0.5 mg/ml), 0.1% (w/v)  $\text{NaN}_3$ , 20 mM HEPES, pH 7.0] for 90 minutes. Endogenous phosphatase activity was quenched by incubating the sections overnight at 65°C. AP activity was detected by using nitroblue tetrazolium chloride (NBT) and 5-bromo-4-chloro-3-indolyl-phosphate-p-toluidine salt (BCIP). Probe intensity in the MGN and retina was quantified on gray-scale images in Scion Image software. For the MGN, a line was drawn along the descending ephrin gradient from the ventral and lateral corner (in coronal section) or anterior and lateral corner (in horizontal section). For the retina, a line was drawn along the retinal ganglion cell layer from nasal to temporal retina. Luminance values were measured, inverted, and scaled from 0 (light; low probe intensity) to 1 (dark; high probe intensity).

### Retrograde labeling of ipsilateral retinal axons

With a picospritzer, we made five injections of Alexa fluor-488-conjugated cholera toxin B subunit (CTB) into the superficial layers of the left superior colliculus of a P0 mouse. A single injection delivered approximately 1  $\mu$ l of CTB. Pups were sacrificed 24 hours after injections. Whole

heads were removed, frozen in isopentane, and sectioned at 20  $\mu$ m on a cryostat. Images of the ipsilateral retina were taken with a Zeiss fluorescent microscope. Pixel intensity values were calculated as described above, without inversion.

### Fluorescent tracing

Adult mice (>6 weeks) were anesthetized with Avertin (320 mg/kg). We injected a saturating volume (2  $\mu$ l) of 1% CTB conjugated to either Alexa fluor-488 or -594 (Molecular Probes, Eugene, OR) into the left and right eyes, respectively. Thus, in the left, rewired, hemisphere, ipsilateral eye projections were labeled green, whereas contralateral eye projections were labeled red. Mice were euthanized 2–3 days after injection by using sodium pentobarbital (50 mg/kg) and were perfused sequentially with phosphate-buffered saline and 4% paraformaldehyde. Brains were removed from the skull, equilibrated in 30% sucrose, and sectioned frozen in the coronal or horizontal plane at 50  $\mu$ m. Sections were imaged by confocal microscopy. The LGd and MGN were identified on representative sections using Alexa-640/660 Nissl stain (Molecular Probes).

### Identification of retinal label in standard sections

To compare the extent and location of retinal label in matched locations within the MGN of wild-type and ephrin knockout mice, the LGd was used as a positional reference to define the anterior, posterior, dorsal, and ventral borders of the MGN. In the coronal plane, retinal projections to the MGN were consistently observed in six serial 50- $\mu$ m sections (labeled “C1–C6,” as indicated on the horizontal schematic shown in Fig. 2E). Section C1, the most anterior section, was defined as the third section rostral to the posterior boundary of the LGd (located at approximately  $-2.8$  bregma). This section and the next (section C2) were used for measuring the amount and extent of retinal label in “anterior” MGN sections. Sections C5 and C6 were used for measuring label in “posterior” MGN sections. In the horizontal plane, rewired projections were consistently observed in at least eight sections (labeled “H1–H8”). The lateral posterior nucleus (LP) lies dorsal to the LGd and MGN and also receives enhanced retinal projections after rewiring. We ensured that projections into the LP were not included in the calculations by conservatively including only six serial sections in our data analysis (Fig. 2A). Section H1 was defined as the most ventral section containing LGd. This section was used for measurements in “ventral” MGN sections. We designated the most dorsal section “H6”; this section was used for measurements in “dorsal” sections.

### Retinal labeling in the MGN

Sections were examined by confocal microscopy to produce eight-bit digital images of red and green fluorescence. Images were normalized to contain gray values of 0–255 for each channel. A region of interest (ROI) encompassing all label in the rewired MGN was defined in Adobe Photoshop for each coronal or horizontal section. The LGd, or in more posterior sections the optic tract, was used as the lateral border for the MGN. The ROI never extended past the medial border of the MGN as determined by Nissl staining on representative sections. To quantify the degree of retinal innervation from the ipsilateral and con-

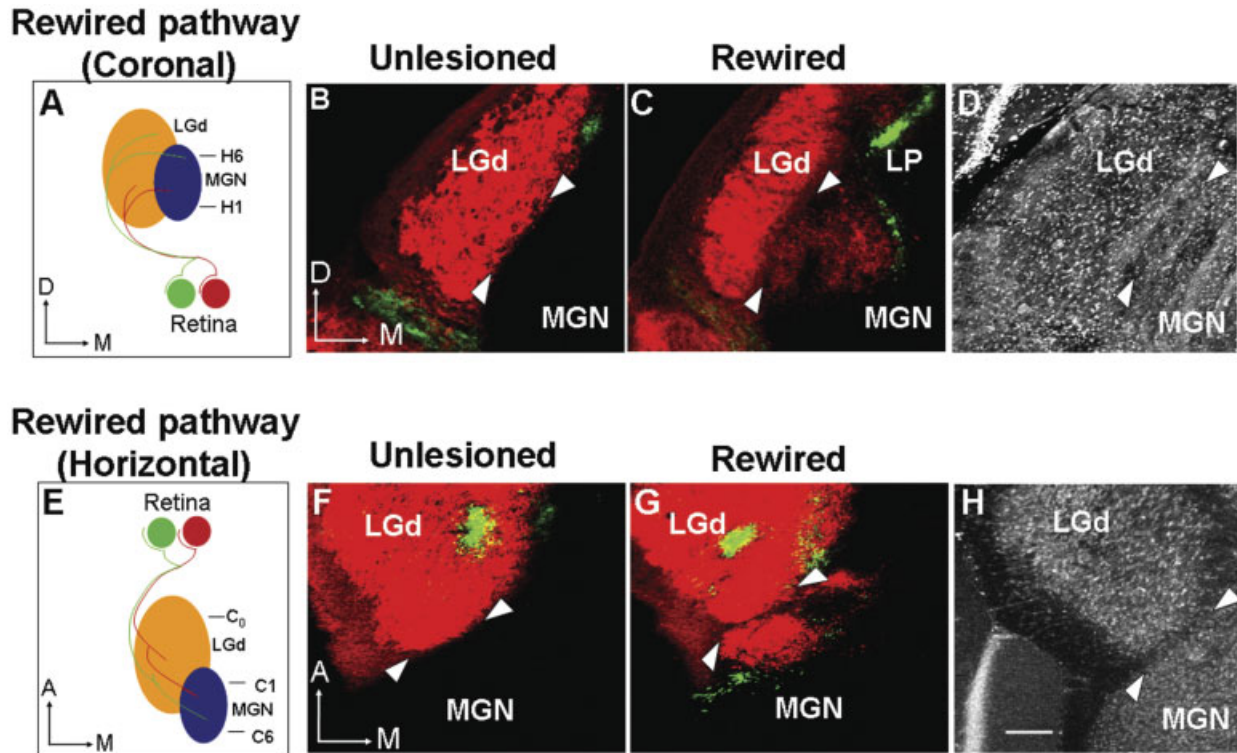


Fig. 2. Rewired projections in coronal (A–D) and horizontal (E–H) sections. A,E: Schematic representation of rewired visual projections in coronal and horizontal sections, respectively. In unlesioned animals, retinal axons innervate the dorsal lateral geniculate nucleus (LGd; orange), whereas auditory input reaches the medial geniculate nucleus (MGN; blue) from the inferior colliculus. In “rewired” animals, deafferentation of the MGN induces retinal axons to innervate the MGN. A: H1 (most ventral) and H6 (most dorsal) mark the approximate locations used for horizontal sections. E: C1 (most anterior) and C6 (most posterior) mark the approximate locations used for coronal sections. C0 marks the approximate location of the LGd section shown in Figure 6. B,C: Representative coronal sections (at level C1) in a

control, unlesioned mouse (B) and a rewired mouse (C). In the rewired mouse, retinal axons can be seen overshooting the medial boundary of the LGd and projecting into the MGN. Enhanced retinal projections are also seen in the lateral posterior nucleus (LP). Retinal axons are labeled with Alexa fluor-conjugated CTB. Contralateral projections are labeled in red. Ipsilateral projections are labeled in green. Arrowheads mark the LGd/MGN boundary. D: Matched Alexa-640/660 Nissl-stained section, thickness 50  $\mu$ m. E–H: Horizontal view and sections. In horizontal sections (at level H6), retinal axons can be seen overshooting the posterior boundary of the LGd. Details are the same as for coronal sections. Scale bar = 0.1 mm in H (applies to B–D, F–H).

tralateral eyes in each ROI, we counted the total number of red and green pixels in each ROI that exceeded a pixel intensity threshold of 200. From these measurements we determined the total number of pixels and the totals in each channel for each ROI. The percentage of ipsilateral pixels was defined as the number of green pixels in that ROI divided by the total number of rewired pixels in the same ROI.

### Location and extent of ipsilateral terminations

For analyzing the location and extent of ipsilateral projections in the LGd and MGN, we analyzed data from five serial coronal sections each from the LGd and the rewired MGN. The most anterior LGd section used in this analysis was the fifth section caudal to the anterior end of LGd (section C0 in Fig. 2E). In some cases, we used the control hemisphere of rewired mice for LGd data. Rewired MGN data included coronal sections C1–C5 as defined above. In NIH ImageJ, a line 45° from horizontal was drawn on each image from the most ventral to the most dorsal retinal projection in the LGd or MGN (see Fig. 6). The smallest region encompassing all green pixels (ipsilateral) was out-

lined by hand. The centroid position of this region was calculated in NIH ImageJ and projected normally onto the 45° line. Relative centroid position was defined as the distance of the centroid from the ventralmost retinal projection, divided by total line length. To measure the spread of ipsilateral label, the most ventral and dorsal ipsilateral label were projected normally onto the 45° line. The relative extent of ipsilateral label was defined as the distance between these ventral and dorsal points divided by the total line length.

## RESULTS

Early in development, retinal fibers traverse the lateral edge of the thalamus via the optic tract en route to the superior colliculus. Subsequently, they branch into the principal visual nucleus of the thalamus, the LGd. In mice, early deafferentation of the MGN causes retinal projections to overshoot the expected medial and posterior boundaries of the LGN and project into this aberrant target (Lyckman et al., 2001; Fig. 2). Coronal sections through the posterior thalamus (Fig. 2A–D) show retinal projections into the LGd in control, unlesioned mice (Fig.

2B) and to the LGd and the MGN in rewired mice (Fig. 2C). Horizontal sections through the thalamus (Fig. 2E–H) show retinal projections to the LGd in unlesioned mice (Fig. 2F) and additionally to the MGN in rewired mice (Fig. 2G). Here, we sought to understand the patterning of retinal projections in the MGN and whether ephrin-A proteins contribute to the specification of this patterning.

### Ephrin expression in the mouse MGN

The mouse MGN shows graded expression of ephrin-A2 and ephrin-A5 mRNAs and ephrin-A proteins, with greatest expression at the ventrolateral border of the MGN (Lyckman et al., 2001). We have confirmed this ephrin-A gradient in coronal sections, showing that it decreases toward the dorsal and medial part of the MGN (Fig. 3A), and have further characterized it in horizontal sections of the MGN at P0. AP staining with an EphA3 affinity probe revealed graded ephrin-A protein expression in horizontal sections. In these sections, the highest ephrin-A expression level was seen at the anterolateral border of the MGN. The expression then decreased posteriorly and medially from this border (Fig. 3B). The high lateral ephrin-A expression in the MGN, seen in both coronal and horizontal sections, abuts either the medial edge of the LGd or, in more posterior sections, the posterior LGd and optic tract. The pattern of ephrin expression is similar in the LGd: ephrin-A2 and -A5 mRNA expression is high at the lateral, ventral, and anterior edge and decreases toward the medial, dorsal, and posterior end (Feldheim et al., 1998). This results in a head-to-tail organization pattern between these two nuclei; low ephrin expression in the LGN abuts high ephrin expression in the MGN. The absence of EphA3-AP staining in the thalamus of ephrin-A2/A5 knockout mice indicates that ephrin-A2 and -A5 account for all the ephrin-A staining in these thalamic nuclei but does not absolutely rule out the presence of other ephrin-A ligands (Feldheim et al., 2000).

### Retinal origin of ipsilateral axons

In wild-type mice, temporal retinal ganglion cell axons express high levels of receptors for ephrin-A2 and ephrin-A5 (EphA3 in chick: Cheng et al., 1995; EphA5 in mice: Feldheim et al., 1998, 2000; Reber et al., 2004). By using an ephrinA5-AP probe, we confirmed that the pattern of receptor expression is the same in ephrin-A2/A5 knockout mice (Fig. 3C,E). We hypothesized that ipsilateral axons, which arise from the temporal retina, would have high levels of receptor expression. To examine this hypothesis, we retrogradely labeled ipsilateral axons from the superior colliculus of wild-type and ephrin-A2/A5 knockout mice ( $n = 2$  animals each). Unilateral injections of CTB in the superior colliculus labeled retinal ganglion cells in the ventrotemporal retina of the same side (Fig. 3D). Comparisons of the receptor staining with corresponding sections of back-labeled retinal neurons demonstrated that ipsilateral projections indeed arose from regions of the retina with high receptor expression. Notably, there was no difference in ipsilaterally projecting retinal ganglion cells between wild-type and ephrin knockout mice (Fig. 3F). EphrinA5-AP probe staining of optic tract axons in whole mounts of the thalamus at P0 revealed robust receptor expression in the entire tract overlaying the LGd, in a manner that paralleled the distribution of retinofugal axons (Lyckman et al., 2001). The axon staining pattern is consistent with the widespread distribution

of axons from diverse parts of the retina within the optic tract (Simon and O'Leary, 1991; Chan and Guillery, 1994; Fitzgibbon and Reese, 1996).

### Effects of ephrin expression on patterning eye-specific projections in the rewired MGN

**Patterning in the anterior-posterior dimension.** Different mean levels of Eph receptor expression in contralateral and ipsilateral retinal ganglion cells indicate that ephrin expression may contribute to eye-specific targeting. For example, ephrin is expressed from a high anterior to low posterior gradient in the MGN (Fig. 3B). Ipsilateral axons, which show high receptor expression, should avoid areas of the MGN with high ligand expression, namely, anterior MGN. We examined eye-specific projections in coronal sections through anterior and posterior MGN (Fig. 4). Intraocular injections of Alexa fluor-488 (green) and -594 (red) CTB were made, respectively, into the left and right eyes of adult, unilaterally rewired mice. In all cases, ipsilateral projections were labeled with green CTB. In rewired wild-type mice, ipsilateral retinal axons consistently avoided areas of high ephrin expression, namely, anterior MGN, and preferentially occupied the posterior region of this nucleus (Fig. 4A–C). We quantified the total number of labeled pixels in the rewired MGN for each section. From this, we calculated the percentage of those pixels that were from the ipsilateral eye (labeled with green CTB). The percentage of rewired axons representing the ipsilateral eye was significantly higher in posterior sections compared with anterior sections (Fig. 4D;  $P < 0.01$ ,  $t$ -test;  $n = 5$  animals; this and all subsequent comparisons treat each animal as a single datum).

To determine whether this patterning is influenced by ephrin expression, we performed the same analysis on ephrin-A2/A5 knockout mice. We suspected that ipsilateral projections would be specifically enhanced in anterior MGN, where ephrin is highly expressed in the wild type (Fig. 4E). Indeed, tracing retinal projections in rewired ephrin-A2/A5 knockout mice revealed ipsilateral patterning that differed from that in the wild type. In these mice, the percentage of ipsilateral label in anterior MGN significantly increased compared with wild type (Fig. 4F). A comparison of matched anterior sections demonstrated significantly more ipsilateral projections in ephrin knockout vs. wild-type mice (Fig. 4D,H;  $P < 0.05$ ,  $t$ -test;  $n = 5$  animals each). Ipsilateral representation in posterior MGN was still higher than that in anterior MGN, but this difference was not significant ( $P > 0.1$ ,  $t$ -test;  $n = 5$  animals). There was no significant change in the amount of ipsilateral representation in matched posterior sections of knockout vs. wild-type mice ( $P > 0.45$ ,  $t$ -test;  $n = 5$  animals each). There were no apparent changes in the patterning of contralateral projections in the rewired MGN of ephrin-A2/A5 knockout mice.

**Patterning in the dorsoventral dimension.** As can be seen in coronal sections, ipsilateral axons not only project more posteriorly within the MGN but also more dorsally and medially than contralateral axons (Fig. 2C). This patterning is also consistent with a repulsive role for the ephrin gradient. In both the LGN and the MGN, ephrin is expressed in a gradient in the dorsoventral dimension, from high ventral to low dorsal (Fig. 3A). With the same reasoning as above, we suspected that ipsilateral axons would preferentially target dorsal MGN (Fig. 5A). To examine this, we analyzed eye-specific projections in

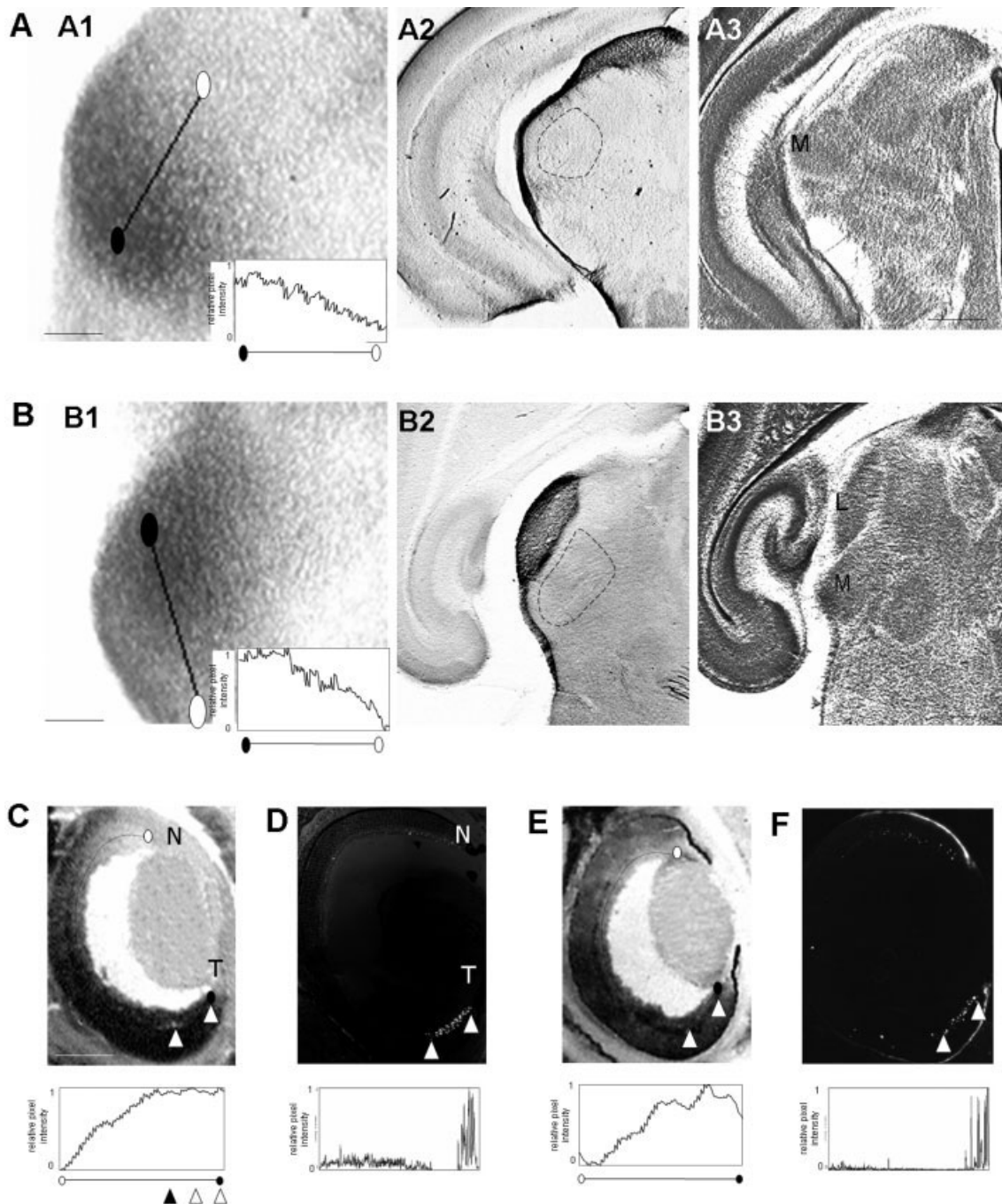


Fig. 3. Ephrin A expression in the MGN (A,B) and EphA expression in the retina (C-F). Coronal (A) and horizontal (B) sections through the wild-type MGN. A1,B1: EphA3-alkaline phosphatase probe staining to show ephrin-A ligand expression in a P0 mouse. **Inset:** Pixel intensity profile of EphA3-AP affinity-probe staining through MGN along the black line from closed to open oval. A2,B2: Matched sections from a P1 mouse with CTB-labeled retinal axons, following bilateral intraocular injection of CTB. Outline marks the boundary of the MGN. A3,B3: Matched sections stained with cresyl violet. L, LGd; M, MGN. C: Ephrin-A affinity-probe staining of a horizontal section through wild-type retina. Temporal retina is located at bottom right (T, temporal; N, nasal). Ipsilaterally projecting cells labeled in D extend from the temporal edge of the retina to the nasal/temporal border, as marked by the two arrowheads. Bottom: Pixel intensity profile of ephrin-A affinity probe staining in the retinal

ganglion cell layer along the dotted line from open to closed oval. The staining intensity from the open arrowhead at the temporal edge to the central arrowhead denotes EphA receptor expression in the ipsilaterally projecting temporal retina; the intensity from the central arrowhead to the solid arrowhead denotes receptor expression in a retinotopically matched binocular zone of the nasal retina that projects contralaterally. (The level of receptor expression is high within both regions, consistent with a possible matched expansion of both projections, and hence of the binocular zone, within the LGd or MGN of ephrin knockout mice.) D: Ipsilaterally projecting retinal ganglion cells, retrogradely labeled with CTB from the superior colliculus. Bottom: Pixel intensity profile of CTB label in the retinal ganglion cell layer. E,F: Same as C,D for ephrin-A2/A5 knockout mice. Scale bars = 0.1 mm in A1,B1; 0.5 mm in A3,B3 (applies to A2,B2,A3,B3); 0.1 mm in C (applies to C-F).

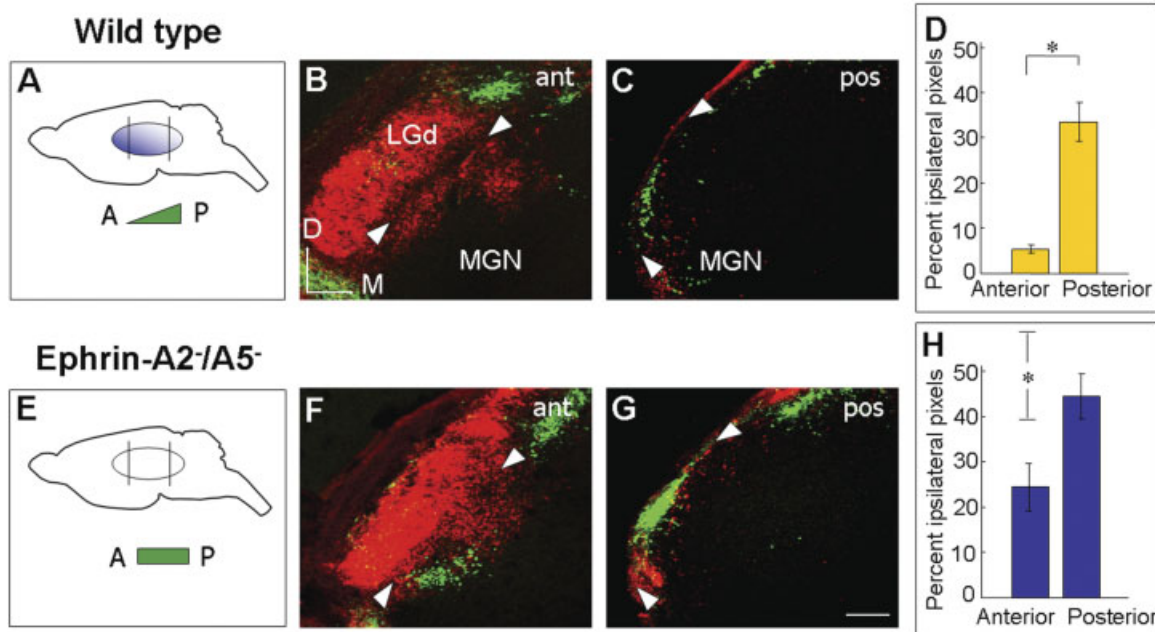


Fig. 4. Anterior-posterior patterning of ipsilateral projections in rewired MGN of wild-type (A–D) and ephrin-A2/A5 double-knockout mice (E–H). A,E: Schematic sagittal section depicting the anteroposterior ephrin gradient in wild-type (A) and ephrin-A2/A5 knockout (E) MGN. Bottom: Corresponding expected distribution of ipsilateral visual projections to the MGN, ranging from anterior (A) to posterior (P). B,C: Coronal sections from a wild-type mouse, showing contralateral projections (red) and ipsilateral projections (green). An anterior

section (at level C1, Fig. 2E) is shown in B; a posterior section (at level C6, Fig. 2E) is shown in C. Arrowheads mark the LGd/MGN boundary. F,G: Similar sections from an ephrin-A2/A5 double-knockout mouse. D,H: Percentage of rewired projections from the ipsilateral eye in anterior and posterior coronal sections, quantified by using confocal images. Error bars show standard errors of the mean. \* $P < 0.05$ . D, wild type; H, ephrin-A2/A5 double knockout. Scale bar = 0.1 mm in G (applies to B,C,F,G).

horizontal sections. In wild-type mice, rewired ipsilateral axons consistently avoided ventral MGN (Fig. 5B), preferring the dorsal part of the nucleus (Fig. 5C). The proportion of ipsilateral label per section was significantly higher in dorsal MGN sections compared with ventral MGN sections (Fig. 5D;  $P < 0.005$ ,  $t$ -test;  $n = 5$  animals). In ephrin-A2/A5 knockout mice, there was a major increase in the proportion of ipsilateral innervation in ventral MGN (Fig. 5E,F). The proportion of ipsilateral label was now much more evenly spread across the nucleus, with little difference between ventral and dorsal sections (Fig. 5H;  $P > 0.2$ ,  $t$ -test;  $n = 5$  animals). The most ventral horizontal sections in ephrin knockout mice received significantly greater ipsilateral innervation than matched sections in wild-type mice (Fig. 5D,H;  $P < 0.01$ ,  $t$ -test;  $n = 5$  animals each).

### Ipsilateral projections in the MGN and LGd of wild-type and ephrin knockout mice

The changes in patterning of ipsilateral projection that we see in the rewired MGN of ephrin knockout mice are reminiscent of the distribution of retinal terminations in normal visual targets, which show similar ephrin expression patterns. For example, in ephrin-A5 knockout mice, temporal axons extend more anteriorly in the LGd (Feldheim et al., 1998). For a more direct comparison, we measured the centroid location of the ipsilateral projection, as well as the spread of ipsilateral label along the axis of ephrin gradient, in both the LGd and the MGN of wild-type and ephrin knockout mice (Fig. 6). We focused our analysis on coronal sections, because the ipsilateral pro-

jection to the LGd is best characterized in this orientation. In wild-type mice, ipsilateral projections target the dorsal and medial edge of the LGd. In ephrin-A2/A5 knockout mice, ipsilateral projections to the LGd spread farther ventrally and laterally and appeared more widespread compared with the wild type (Fig. 6A). Our metrics demonstrate that, in the LGd of ephrin knockout mice, the ipsilateral projection shifted significantly ventrally (Fig. 6B;  $P < 0.01$ ,  $t$ -test;  $n = 5$  animals each) and tended to spread farther along the dorsoventral dimension (Fig. 6C;  $P < 0.09$ ,  $t$ -test;  $n = 5$  animals each) compared with wild type. Such spread is expected in the LGd of knockout mice if high ventrolateral ephrin expression constrains ipsilateral axons in the wild type. We compared this shift in patterning to the position and spread of ipsilateral label along the ephrin gradient axis in the rewired MGN (Fig. 6D). Here, the centroid of the ipsilateral label also shifted significantly (Fig. 6E;  $P < 0.05$ ,  $t$ -test;  $n = 5$  animals each) and tended to spread farther ventrally (Fig. 6F;  $P < 0.07$ ,  $t$ -test;  $n = 5$  animals each) in knockout mice compared with wild type. These data, derived from coronal sections, are consistent with the horizontal sections shown in Figure 5. In fact, the shift and spread of the ipsilateral label in ephrin knockout mice appeared to be even more pronounced in the rewired MGN compared with the LGd.

### Spread of retino-MGN terminations in wild-type and ephrin knockout mice

In a previous study, Lyckman et al. (2001) demonstrated that retino-MGN projections are more extensive in ephrin-A2/A5 knockout mice compared with wild type,

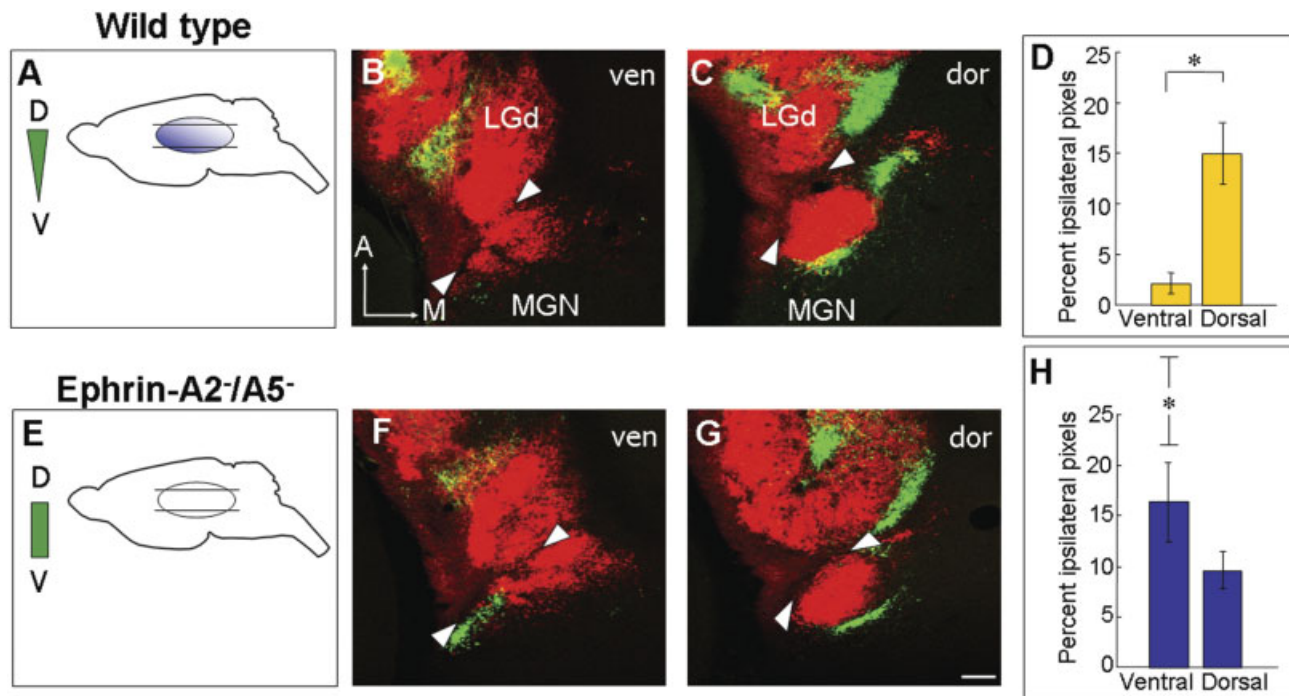


Fig. 5. Dorsal-ventral patterning of ipsilateral projections in rewired MGN of wild-type (A–D) and ephrin-A2/A5 double-knockout mice (E–H). A,E: Schematic sagittal section depicting the dorsoventral ephrin gradient in wild-type (A) and ephrin-A2/A5 double-knockout (E) MGN. Left: Corresponding expected distribution of ipsilateral visual projections to the MGN, ranging from dorsal (D) to ventral (V). B,C: Horizontal sections from a wild-type mouse, showing contralateral projections (red) and ipsilateral projections (green). A

ventral section (at level H1, Fig. 2A) is shown in B; a dorsal section (at level H6, Fig. 2A) is shown in C. Arrowheads mark the LGd/MGN boundary. F,G: Similar sections from an ephrin-A2/A5 double-knockout mouse. D,H: Percentage of rewired projections from the ipsilateral eye in ventral and dorsal horizontal sections, quantified by using confocal images. Error bars show standard errors of the mean. \* $P < 0.05$ . D, wild type; H, ephrin-A2/A5 double knockout. Scale bar = 0.1 mm in G (applies to B,C,F,G).

although the relative contributions of ipsilateral and contralateral retinal projections were not evaluated. Here, we also found a roughly twofold increase in the total number of labeled pixels in the rewired MGN of ephrin-A2/A5 knockout mice compared with wild type (Fig. 7, circles;  $P < 0.05$ ,  $t$ -test;  $n = 10$  animals each). This increase was evident despite any obvious differences in cell number or density in the deafferented MGN of these strains, as determined by cell counts from Nissl sections. Our results described so far suggested that ipsilateral projections were specifically increased in knockout mice. We asked whether an increase in the total number of rewired terminals in the knockout mice vs. the wild type could be accounted for solely by an increase in ipsilateral terminals. We calculated, per mouse, the average number of ipsilateral and contralateral pixels in the rewired MGN of wild-type and knockout mice. There was an increase in the extent of contralateral projections between knockout and wild-type mice, although it was not significant ( $P > 0.35$ ,  $t$ -test;  $n = 10$  animals each). There was a much greater, roughly fourfold, increase in the total number of ipsilateral projections in knockout compared with wild-type mice ( $P < 0.001$ ,  $t$ -test;  $n = 10$  animals each). Thus the increase in retinal innervation of the MGN in ephrin-A2/A5 knockout mice is due significantly to an increase in ipsilateral input.

### Interocular segregation in the rewired MGN

In mice, not only are projections from each eye targeted to characteristic eye-specific zones within the LGd but also

ipsilateral and contralateral projections show little to no overlap of termination at the boundaries between these zones. Eye-specific segregation into small focal clusters is observed in the rewired MGN of ferrets, although stereotyped eye-specific zones are not observed (Angelucci et al., 1997). Here, we used dual-color (red and green) intraocular injections, as described above, to examine the extent of segregation of retino-MGN projections in wild-type and ephrin knockout mice. The extent of overlap from the two eyes is indicated by the presence of yellow pixels. Our data indicated that retino-MGN projections were well segregated in wild-type mice: only 0.9% of pixels showed overlap between projections from the two eyes. The degree of eye segregation in rewired retino-MGN projections was comparable to that of normal retino-LGd projections (e.g., Figs. 2, 6), where, with our measure, 0.02% of pixels showed interocular overlap. In rewired ephrin-A2/A5 knockout mice, ipsilateral axons projected more widely in the MGN. However, the changes in ipsilateral targeting did not lead to an increase in the overlap of projections (Figs. 4, 5): 1.3% of pixels showed overlap, a proportion not different from that in rewired wild-type mice ( $P > 0.1$ ,  $t$ -test;  $n = 5$  animals each). Similarly, in the LGd of ephrin knockout mice, 0.1% of pixels showed overlap between the two eyes, which was similar to the proportion in wild-type mice ( $P > 0.05$ ,  $t$ -test;  $n = 5$  animals each). Thus, in agreement with more detailed studies of the LGd (D.A.F., unpublished observations), whereas the size and extent of eye-specific projection zones were significantly influenced

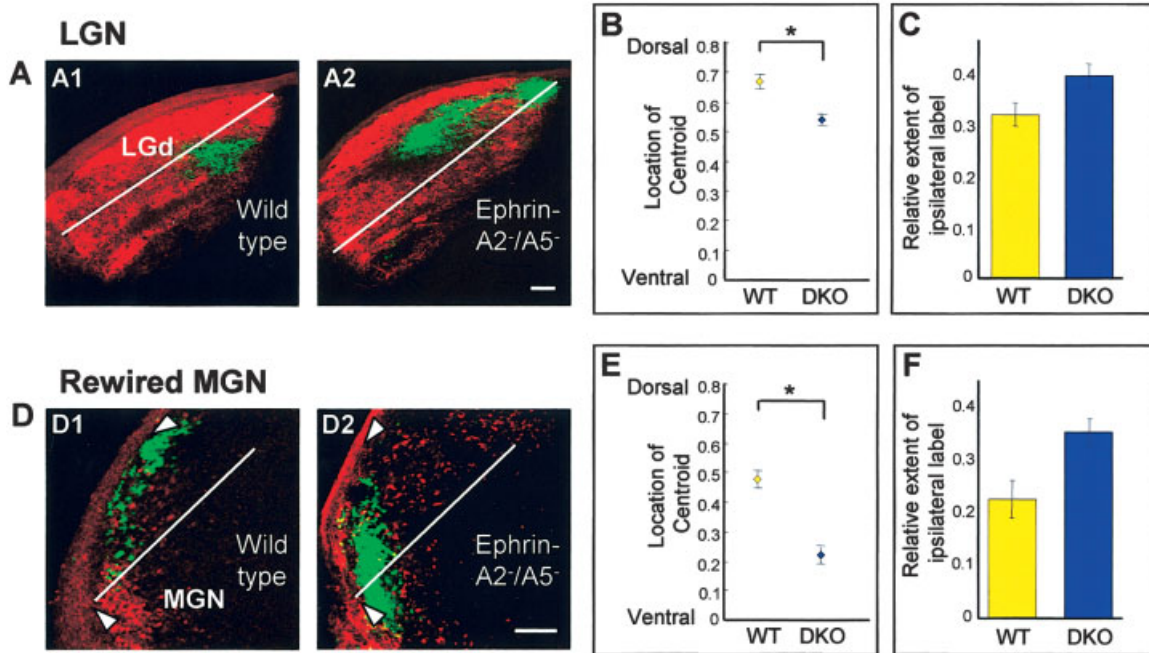


Fig. 6. Comparison of dorsoventral patterning of ipsilateral projections in the LGd (A–C) and rewired MGN (D–F) of wild-type and ephrin-A2/A5 double-knockout mice. A: Representative coronal sections through the LGd (at level C0, Fig. 2H) in wild-type (A1) and ephrin-A2/A5 knockout mice (A2). D: Similar sections through the rewired MGN (at level C5). Line in each figure represents the ephrin gradient in wild-type mice, from high ventral to low dorsal. B,E: Dorsoventral position of ipsilateral centroid in LGd (B) and rewired MGN (E) of wild-type mice (yellow circle) and ephrin-A2/A5 double-

knockout mice (blue circle). Y-axis represents the position of the ipsilateral centroid as a fraction of the full length of retinal projection along the ephrin gradient (0 = most ventral projection, 1 = most dorsal projection). C,F: Spread of ipsilateral projection in the LGd and rewired MGN of wild-type (yellow) and ephrin-A2/A5 double-knockout (blue) mice. Y-axis represents the length of ipsilateral representation along the ephrin gradient as a fraction of the full length of retinal projection along the same gradient. Error bars show standard errors of the mean. \* $P < 0.05$ . Scale bars = 0.1 mm in A,D.

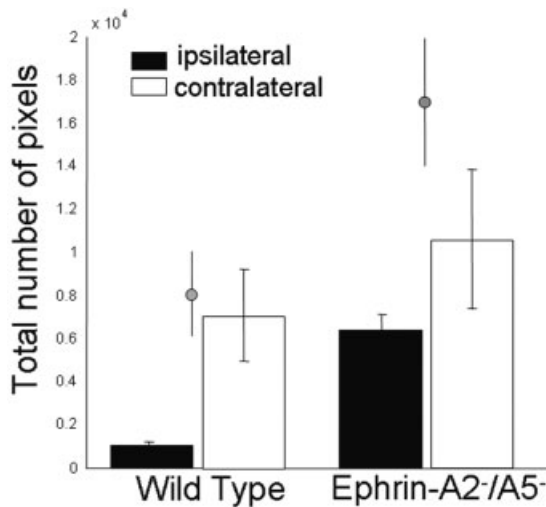


Fig. 7. Ipsilateral and contralateral projections, and total retinal innervation, in the rewired MGN of wild-type and ephrin-A2/A5 double-knockout mice. Bar graphs: wild type (left), ephrin-A2/A5 knockout (right). Open bars depict the average number of ipsilateral pixels in the rewired MGN per mouse. Solid bars depict the average number of contralateral pixels. Circles represent the total number of labeled pixels per mouse in the rewired MGN in wild-type and ephrin knockout mice. Error bars show standard errors of the mean.

by ephrin expression, the overlap and segregation of eye-specific terminals were not.

## DISCUSSION

We have confirmed that there is a graded pattern of ephrin-A protein expression in the mouse MGN that is similar in orientation and expression levels to that in the LGd. High ephrin-A expression in the MGN occurs at the border of the LGd and optic tract. Ipsilaterally projecting retinal ganglion cells express high levels of EphA receptor, and their axons develop highly stereotyped patterns of innervation in wild-type mice, avoiding areas of high ephrin-A expression in the MGN and LGd. In rewired animals, ipsilateral axons preferentially target posterior, dorsal, and medial MGN. The targeting of ipsilateral axons to the MGN and LGd is significantly altered in location and extent in ephrin-A2/A5 knockout mice, suggesting that the ephrin-A gradients are necessary for the establishment of this pattern (Fig. 1). This change in targeting also results in an overall increase in ipsilateral representation in the rewired MGN of ephrin knockout mice compared with wild type. We posit that a specific increase in ipsilateral projections may account in large measure for the expansion of rewired projections previously reported for ephrin knockout mice. Our data suggest that graded topographic labels, such as the ephrins, can serve to shape multiple aspects of afferent patterning, including topographic mapping and the extent and spread of eye-

specific projections, and can do so in both normal and novel targets.

### Patterning of multiple modalities by ephrin/Eph interaction

There is substantial evidence that repulsive interactions between EphA receptors and ephrin-A ligands are crucial in setting up topographic mapping in central visual structures (see the introductory paragraphs). Although the level of EphA receptors on axons of temporal retinal ganglion cells is difficult to establish *in vivo*, *in vitro* assays show that temporal axons from mice lacking the intracellular domain of the EphA5 receptor lose their responsiveness to posterior superior colliculus membranes (Feldheim et al., 2004), demonstrating a requirement for the intracellular domain in the signaling response to topographic cues. Furthermore, retinotectal targeting *in vivo* is disrupted in these mice, demonstrating a requirement for endogenous EphA receptors in topographic mapping. Our present findings suggest a complementary requirement for ephrin-A, and hence for EphA/ephrin-A interactions, in retinofugal mapping within diverse targets.

Sensory axons faithfully reach their appropriate subcortical targets; once there, they develop modality-specific patterns of innervation. Results from previous rewiring experiments have been used to suggest a role for patterned sensory activity in the fine tuning of connections, including retinotopy and eye segregation (Pallas et al., 1990; Angelucci et al., 1997). It has also been suggested that the patterning of rewired projections indicates a role for interactions among developing axons as a key factor in organizing orderly connections (Frost, 1981). Our data, however, offer an additional hypothesis: molecular cues common to the visual and auditory pathway are available to shape patterning of novel retinal projections in auditory targets. Although this paper focuses on the auditory thalamus, similar graded ephrin expression is seen in the somatosensory thalamus and cortex. This expression influences the establishment of a somatotopic map in S1 (Prakash et al., 2000; Vanderhaeghen et al., 2000). Visual axons can also be induced to innervate the ventrobasal nucleus, which traditionally receives somatosensory input (Frost, 1984; Frost and Metin, 1985). The retinotopic map that develops in the rewired somatosensory thalamus may also be influenced by the ephrin/Eph interaction.

In addition to offering an explanation for the patterning of aberrant cross-modal projections, our findings demonstrate a direct and simple way in which multimodal maps may be aligned within a target during normal development. Sensitivity to a common molecular signaling system would provide a parsimonious mechanism to align multiple input pathways, as occurs in the superior colliculus. Although there is less information on direct ephrin involvement in the auditory pathway, the EphA4 receptor and ephrin-B2 ligand are expressed along the tonotopic axis in the chick auditory brainstem (Cramer et al., 2002; Person et al., 2004). Ephrin expression in the mouse inner ear (Pickles et al., 2002; Pickles, 2003), along with the graded ephrin expression shown here, indicates that the ephrins likely participate in axon guidance in regions of the developing auditory pathway as well. The ephrins are also expressed in multiple sensory pathways in the developing cortex (Dufour et al., 2003; Yun et al., 2003). Thus, we suspect that Eph/ephrin interactions may also serve to align multimodal input in higher cortical areas.

### Ephrins and compartmentalization in the developing thalamus

Deafferentation of the MGN leads to increased retinal innervation in ephrin-A2/A5 knockout mice compared with wild-type mice. Together with the high expression of ephrin-A at the border of the MGN and LGd, this finding suggests that the ephrins may contribute to specifying nuclear boundaries in the thalamus. However, retinal axons do not project into the MGN in ephrin knockout mice without deafferentation surgery (present results; Lyckman et al., 2001), demonstrating that the ephrin boundary is not the sole factor in compartmentalization and target selection. A similarly high level of ephrin-A expression is seen at the boundary of the superior and inferior colliculus. In wild-type and ephrin-A5 knockout mice, visual axons initially overshoot the posterior border of the superior colliculus and project into the inferior colliculus (unpublished observations). In ephrin-A5 knockout mice, compared with wild type, significantly more temporal axons extend into the inferior colliculus, indicating that high ephrin expression normally limits this anomalous projection. However, by P14, these projections disappear in both mice, indicating that the auditory brainstem does not support this visual input. In the case of retinal projections to the MGN, early transient projections do not exist; rather, deafferentation of the MGN is necessary to induce retinal axons to sprout into this novel target. These findings together support the idea that sensory axons have an *a priori* competitive advantage in their intended thalamic target, likely originating from molecular cues that are differentially expressed in different thalamic nuclei. It is as yet unclear why deafferentation permits an anomalous input to sprout into the MGN, but insight may come from the vast literature on deafferentation-induced sprouting in the developing and adult brain (see, e.g., Deller and Frotscher, 1997).

We have demonstrated a major increase in ipsilateral retino-MGN input in ephrin-A2/A5 knockout mice. An enhanced ipsilateral retino-MGN projection might arise from additional axons overshooting the LGN/MGN boundary in ephrin knockout mice compared with wild type or from increased arborization of retinal afferents within the MGN. That is, disruption of ephrin expression within the MGN may permit a *constant* number of rewired retinal axons to diverge and innervate areas of the MGN previously avoided, causing an enhancement of the ipsilateral termination zone. This hypothesis is also supported by the spread of ipsilateral terminations seen in the LGd of ephrin-A2/A5 knockout mice. If so, this suggests that targets directly influence the degree of afferent arborization and that presynaptic neurons can have a variable, rather than constant, extent of terminal arbor (Schneider, 1973).

In the LGd of ephrin-A2/A5 knockout mice, expansion of the ipsilateral projection appears to be accompanied by an expansion of the retinotopically matched contralateral projection: Figure 3C (see legend) shows that EphA receptor levels are high in both retinal regions (see also Reber et al., 2004), so that removing the ephrin gradient in the LGd can cause both projections to expand. As a result, we expect that the binocular segment of the LGd would expand whereas the monocular segment would concomitantly shrink in ephrin knockout mice. Indeed, optical imaging of primary visual cortex in ephrin-A2/A5 knockout mice demonstrates an expansion of binocular cortex and a contraction of monocular

cortex (Newton et al., 2004), likely resulting from changes in retino-LGd projections. In the MGN of knockout mice, there is a significant expansion of ipsilateral projections and also a moderate expansion of contralateral projections (Fig. 7). It is possible that, in the MGN, expansion of the ipsilateral (or binocular) input has less influence on the monocular input—perhaps due to a more complex competition for space within the deafferented MGN. Unlike the case in the LGd, where expansion of the binocular zone necessarily reduces the monocular zone within a nucleus that is fully innervated by the retina, retinal axons in the deafferented MGN also compete for space with remaining normal inputs and with other novel inputs (Angelucci et al., 1998). It is likely that some inputs must shrink as a result of the ipsilateral expansion, but it is less clear that this will be the contralateral monocular input.

### Ephrins and eye-specific segregation

We find that, in ephrin-A2/A5 knockout mice, the ipsilateral retinal zone is displaced and extended in both the rewired MGN and the LGd; however, the terminations remain sharply clustered and show no greater overlap than in wild-type mice. Thus, local segregation between terminals from the two eyes is unaffected. These data are consistent with the hypothesis that the formation of large-scale eye-specific layers and local interocular segregation are dissociable processes (Huberman et al., 2002; Muir-Robinson et al., 2002). It is likely that the former process requires the presence of specific labeling molecules, whereas the local segregation of eye-specific terminations may be driven by a separate mechanism, such as synchronous electrical activity in retinal ganglion cells of either eye. Similarly, retinal terminations from the two eyes in the MGN of rewired ferrets initially overlap extensively, and progressively segregate into small eye-specific clusters (Angelucci et al., 1997). However, they do not form eye-specific layers similar to those in the LGd (Hahm et al., 1999). It is likely that additional cues, likely molecular ones, are necessary to guide the complex lamination seen in the ferret LGN and that these cues are not present in the MGN.

These considerations indicate that the organization of retinal inputs into eye-specific regions involves several mechanisms. We show that topographic mapping labels, such as the ephrins, are integrally involved in regulating the size and extent of ipsilateral projections and can do so in normal and novel targets of the retina. Local nonoverlapping segregation of inputs from the two eyes may arise from correlated electrical activity. The large-scale laminar pattern of eye-specific segregation and the location of eye-specific layers likely relates to molecular differences between temporal and nasal retinal axons and their target zones, including EphA/ephrin-A levels (Reber et al., 2004; Hansen et al., 2004). The fact that both the LGd and the MGN in mice exhibit eye-specific lamination indicates that such molecular cues must be present in both normal and novel targets. These cues persist in the absence of ephrin-A2 and -A5, as evident from the persistence of eye-specific lamination in the LGd and MGN of knockout mice. The nature of these cues and how they interact with Eph receptors and ephrin ligands remain to be determined.

### ACKNOWLEDGMENTS

We thank Christine Waite and Monique Brouillette for technical assistance, and Sonal Jhaveri for advice.

### LITERATURE CITED

- Angelucci A, Clasca F, Bricolo E, Cramer KS, Sur M. 1997. Experimentally induced retinal projections to the ferret auditory thalamus: development of clustered eye-specific patterns in a novel target. *J Neurosci* 17:2040–2055.
- Angelucci A, Clasca F, Sur M. 1998. Brainstem inputs to the ferret medial geniculate nucleus and the effect of early deafferentation on novel retinal projections to the auditory thalamus. *J Comp Neurol* 400:417–439.
- Chan SO, Guillery RW. 1994. Changes in fiber order in the optic nerve and tract of rat embryos. *J Comp Neurol* 344:20–32.
- Cheng HJ, Nakamoto M, Bergemann AD, Flanagan JG. 1995. Complementary gradients in expression and binding of ELF-1 and Mek4 in development of the topographic retinotectal projection map. *Cell* 82:371–381.
- Cramer KS, Karam SD, Bothwell M, Cerretti DP, Pasquale EB, Rubel EW. 2002. Expression of EphB receptors and EphrinB ligands in the developing chick auditory brainstem. *J Comp Neurol* 452:51–64.
- Deller T, Frotscher M. 1997. Lesion-induced plasticity of central neurons: sprouting of single fibres in the rat hippocampus after unilateral entorhinal cortex lesion. *Prog Neurobiol* 53:687–727.
- Drescher U, Kremoser C, Handwerker C, Loschinger J, Noda M, Bonhoeffer F. 1995. In vitro guidance of retinal ganglion cell axons by RAGS, a 25 kDa tectal protein related to ligands for Eph receptor tyrosine kinases. *Cell* 82:359–370.
- Dufour A, Seibt J, Passante L, Depaepe V, Ciossek T, Frisen J, Kullander K, Flanagan JG, Polleux F, Vanderhaeghen P. 2003. Area specificity and topography of thalamocortical projections are controlled by ephrin/Eph genes. *Neuron* 39:453–465.
- Feldheim DA, Vanderhaeghen P, Hansen MJ, Frisen J, Lu Q, Barbacid M, Flanagan JG. 1998. Topographic guidance labels in a sensory projection to the forebrain. *Neuron* 21:1303–1313.
- Feldheim DA, Kim YI, Bergemann AD, Frisen J, Barbacid M, Flanagan JG. 2000. Genetic analysis of ephrin-A2 and ephrin-A5 shows their requirement in multiple aspects of retinocollicular mapping. *Neuron* 25:563–574.
- Feldheim DA, Nakamoto M, Osterfield M, Gale NW, DeChiara TM, Rohatgi R, Yancopoulos GD, Flanagan JG. 2004. Loss-of-function analysis of EphA receptors in retinotectal mapping. *J Neurosci* 24:2542–2550.
- Fitzgibbon T, Reese BE. 1996. Organization of retinal ganglion cell axons in the optic fiber layer and nerve of fetal ferrets. *Vis Neurosci* 13:847–861.
- Flanagan JG, Cheng HJ, Feldheim DA, Hattori M, Lu Q, Vanderhaeghen P. 2000. Alkaline phosphatase fusions of ligands or receptors as in situ probes for staining of cells, tissues, and embryos. *Methods Enzymol* 327:19–35.
- Frisen J, Yates PA, McLaughlin T, Friedman GC, O'Leary DD, Barbacid M. 1998. Ephrin-A5 (AL-1/RAGS) is essential for proper retinal axon guidance and topographic mapping in the mammalian visual system. *Neuron* 20:235–243.
- Frost DO. 1981. Orderly anomalous retinal projections to the medial geniculate, ventrobasal, and lateral posterior nuclei of the hamster. *J Comp Neurol* 203:227–256.
- Frost DO. 1984. Axonal growth and target selection during development: retinal projections to the ventrobasal complex and other “nonvisual” structures in neonatal Syrian hamsters. *J Comp Neurol* 230:576–592.
- Frost DO, Metin C. 1985. Induction of functional retinal projections to the somatosensory system. *Nature* 317:162–164.
- Hahm JO, Cramer KS, Sur M. 1999. Pattern formation by retinal afferents in the ferret lateral geniculate nucleus: developmental segregation and the role of N-methyl-D-aspartate receptors. *J Comp Neurol* 411:327–345.
- Hansen MJ, Dallal GE, Flanagan JG. 2004. Retinal axon response to ephrin-As shows a graded, concentration-dependent transition from growth promotion to inhibition. *Neuron* 42:717–730.
- Huberman AD, Stellwagen D, Chapman B. 2002. Decoupling eye-specific segregation from lamination in the lateral geniculate nucleus. *J Neurosci* 22:9419–9429.
- Lyckman AW, Jhaveri S, Feldheim DA, Vanderhaeghen P, Flanagan JG,

- Sur M. 2001. Enhanced plasticity of retinthalamic projections in an ephrin-A2/A5 double mutant. *J Neurosci* 21:7684–7690.
- Monnier PP, Sierra A, Macchi P, Deitinghoff L, Andersen JS, Mann M, Flad M, Hornberger MR, Stahl B, Bonhoeffer F, Mueller BK. 2002. RGM is a repulsive guidance molecule for retinal axons. *Nature* 419:392–395.
- Monschau B, Kremoser C, Ohta K, Tanaka H, Kaneko T, Yamada T, Handwerker C, Hornberger MR, Loschinger J, Pasquale EB, Siever DA, Verderame MF, Muller BK, Bonhoeffer F, Drescher U. 1997. Shared and distinct functions of RAGS and ELF-1 in guiding retinal axons. *EMBO J* 16:1258–1267.
- Muir-Robinson G, Hwang BJ, Feller MB. 2002. Retinogeniculate axons undergo eye-specific segregation in the absence of eye-specific layers. *J Neurosci* 22:5259–5264.
- Nakagawa S, Brennan C, Johnson KG, Shewan D, Harris WA, Holt CE. 2000. Ephrin-B regulates the ipsilateral routing of retinal axons at the optic chiasm. *Neuron* 25:599–610.
- Newton JR, Sharma J, Yu H, Sur M. 2004. Intrinsic signal optical imaging reveals the distinct effects of thalamic and cortical mechanisms on patterning and arealization in V1 and V2 of ephrin A2/A5 knock-out mice. 2004 Abstract Viewer and Itinerary Planner. Washington, DC: Society for Neuroscience.
- O'Leary DD, McLaughlin T. 2005. Mechanisms of retinotopic map development: Ephs, ephrins, and spontaneous correlated retinal activity. *Prog Brain Res* 147:43–65.
- Pallas SL, Roe AW, Sur M. 1990. Visual projections induced into the auditory pathway of ferrets. I. Novel inputs to primary auditory cortex (AI) from the LP/pulvinar complex and the topography of the MGN-AI projection. *J Comp Neurol* 298:50–68.
- Person AL, Pat Cerretti D, Pasquale EB, Rubel EW, Cramer KS. 2004. Tonotopic gradients of Eph family proteins in the chick nucleus laminaris during synaptogenesis. *J Neurobiol* 60:28–39.
- Pickles JO. 2003. Expression of Ephs and ephrins in developing mouse inner ear. *Hear Res* 178:44–51.
- Pickles JO, Claxton C, Van Heumen WR. 2002. Complementary and layered expression of Ephs and ephrins in developing mouse inner ear. *J Comp Neurol* 449:207–216.
- Prakash N, Vanderhaeghen P, Cohen-Cory S, Frisen J, Flanagan JG, Frostig RD. 2000. Malformation of the functional organization of somatosensory cortex in adult ephrin-A5 knock-out mice revealed by in vivo functional imaging. *J Neurosci* 20:5841–5847.
- Reber M, Burrula P, Lemke G. 2004. A relative signalling model for the formation of a topographic neural map. *Nature* 431:847–853.
- Roe AW, Pallas SL, Hahm JO, Sur M. 1990. A map of visual space induced in primary auditory cortex. *Science* 250:818–820.
- Schneider GE. 1973. Early lesions of superior colliculus: factors affecting the formation of abnormal retinal projections. *Brain Behav Evol* 8:73–109.
- Sharma J, Angelucci A, Sur M. 2000. Induction of visual orientation modules in auditory cortex. *Nature* 404:841–847.
- Simon DK, O'Leary DD. 1991. Relationship of retinotopic ordering of axons in the optic pathway to the formation of visual maps in central targets. *J Comp Neurol* 307:393–404.
- Sur M. 2004. Rewiring cortex: cross-modal plasticity and its implications for cortical development and function. In: Calvert GA, Spence C, Stein BE, editors. *The Handbook of Multisensory Processes*. Cambridge: MIT Press. p 681–694.
- Sur M, Garraghty PE, Roe AW. 1988. Experimentally induced visual projections into auditory thalamus and cortex. *Science* 242:1437–1441.
- Sur M, Leamey C. 2001. Development and plasticity of cortical areas and networks. *Nature Rev Neurosci* 2:251–262.
- Vanderhaeghen P, Lu Q, Prakash N, Frisen J, Walsh CA, Frostig RD, Flanagan JG. 2000. A mapping label required for normal scale of body representation in the cortex. *Nat Neurosci* 3:358–365.
- Williams SE, Mann F, Erskine L, Sakurai T, Wei S, Rossi DJ, Gale NW, Holt CE, Mason CA, Henkemeyer M. 2003. Ephrin-B2 and EphB1 mediate retinal axon divergence at the optic chiasm. *Neuron* 39:919–935.
- Yates PA, Roskies AL, McLaughlin T, O'Leary DD. 2001. Topographic-specific axon branching controlled by ephrin-As is the critical event in retinotectal map development. *J Neurosci* 21:8548–8563.
- Yun ME, Johnson RR, Antic A, Donoghue MJ. 2003. EphA family gene expression in the developing mouse neocortex: regional patterns reveal intrinsic programs and extrinsic influence. *J Comp Neurol* 456:203–216.